

CMA6 Fig. 2 Photocurrent line scan of a 50-stripe SIN broad-area high-power LDA (10 W device) emitting at 1.53 eV photon energy (808 nm) for front-facet illumination before and after 24 h operation at 20 A and $T = 20^\circ\text{C}$. The excitation energy was 1.32 eV, i.e., below the effective band gap of the structure. The initial defect distribution already shows a modulation, which is due to nonuniform strain relaxation. The defect distribution after 24 h of operation reveals defect accumulation at the positions of the emitters.

the PC spectrum. This behavior provides an excellent *measure of the aging status* in the early stages of the aging process of an individual device as discussed in detail in the framework of the changes of the vertical current transport mechanisms. The whole behavior is discussed on the basis of model calculations. Note that the lowering of the ratio for high photon energies ($E \approx 3$ eV) is due to aging enhanced surface recombination. Thus mapping of the array at a defined wavelength permits the monitoring of all these processes independently. As an example, maps of the evolution of the defect band are depicted in Fig. 2.

We have applied a number of techniques, including PC analysis, to monitor the gradual processes that accompany the operation of LDA. The results concern microscopic aging mechanisms and ways to obtain failure prediction techniques for individual LDA. The latter findings could be of utmost relevance for pre-selecting devices with reduced expected lifetime.

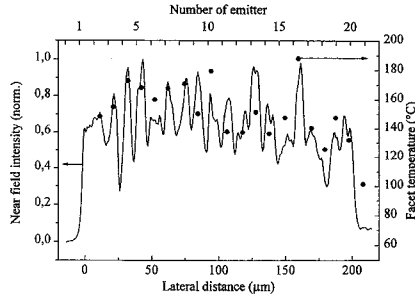
*Jenoptik Laserdiode GmbH, Prüssingstr.41, D-07745 Jena, Germany

CMA7 9:45 am

Facet temperature limits of GaAlAs/GaAs high-power laser diode arrays

R. Puchert, A. Bärwolff, J. W. Tomm, U. Menzel, A. Lau, M. Voß, *Max-Born-Institut für Nichtlineare Optik und Kurzzeitspektroskopie, Rudower Chaussee 6, 12489 Berlin, Germany*

Catastrophical optical damage (COD) is one of the main reasons for emitter failures in high-power laser diode arrays (LDAs). Interaction processes between emitters can cause serious damage to the whole device thereby limiting reliability and lifetime of the LDA. Further insight into the microscopic processes that accompany the COD process can be gathered by facet temperature measurements for operation conditions close to the COD level.¹ These measurements provide for the first time the possibility of quantification of the processes related to the COD process.



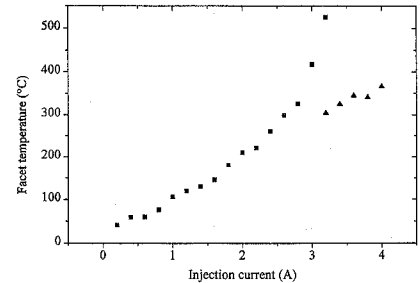
CMA7 Fig. 1 Lateral near-field intensity (solid line) and facet temperatures (full circles) for all emitters of a 20-stripe high-power GaAlAs/GaAs LDA for an injection current of 1.7 A and an output power of 0.89 W respectively. Threshold current: 0.53 A; Heat sink temperature: 25°C .

The LDA investigated are 20-stripe double quantum well (DQW) graded index separate confinement heterostructures (GRIN-SCH) emitting about 1 W cw at 1.5 A operation current. The emission wavelength is 808 nm. The resonator has an asymmetric design, the front facet is coated with a Al_2O_3 $\lambda/4$ antireflection coating.

Facet temperatures were measured with a micro-Raman setup, providing a spatial resolution of 1.5 μm . Typical excitation power levels realized by a 488-nm Argon ion laser line are 850 μW . The facet surface temperature is derived from the ratio between Stokes and anti-Stokes lines of the GaAs-like TO phonons, which exclusively arise from the DQW region. Additionally near-field intensity distributions and output power were monitored for the same high-load operation conditions close to the COD level.

Typical near-field distributions are depicted in Fig. 1. Micro-Raman data on facet temperatures of the corresponding emitters are added. The general shape of both near-field distribution and facet temperature corresponds well. Note, that the facet temperature rise as a result of reabsorption of emitted photons near the facets is locally very different and depends on the near field intensity.¹ This leads to the conclusion that facet overheating does not necessarily occur in the central region of the LDA.

Figure 2 displays micro-Raman facet temperatures versus injection current. For this experiment the temperature of a single emitter situated in center of the array was determined. Up to an operation current of $I = 2.8$ A ($P = 1.73$ W), which exceeds the standard level by 40%, the facet temperature increases linearly. For larger current a superlinear dependence is observed and indicates the approach to the COD level. For $I = 3.2$ A and output power corresponding to an effective power density of 1 MW/cm^2 we directly monitored the COD process and observed a peak temperature of 525°C . To our knowledge this is the highest value experimentally observed so far. Note that the observed power density is about one order of magnitude lower than the established value of about 10 MW/cm^2 .^{2,3} For further increasing currents the facet temperature is dramatically reduced because the optical feed-back ended for the failed emitter. The further linear tem-



CMA7 Fig. 2 Facet temperature obtained by micro-Raman measurements as a function of injection current for a 20-stripe high-power GaAlAs/GaAs LDA. The temperature was measured in the center of the emitters (■—facet temperature before the emitter failure, ▲—facet temperature after the emitter failure). Threshold current: 0.53 A; Heat sink temperature: 25°C .

perature increase is the result of the thermal coupling to the neighbors. This result is discussed for a theoretical model to describe the facet heating in terms of recombination and absorption mechanisms.

1. R. Puchert, A. Bärwolff, U. Menzel, A. Lau, M. Voß, T. Elsaesser, *J. Appl. Phys.* **80**, 5559 (1996).
2. F. Kappeler, K. Mettler, K.-H. Zschauer, in *Proc. IEE* **129** (December 1982).
3. J. S. Yoo, H. H. Lee, P. S. Zory, *IEEE Photon. Technol. Lett.* **3** (July 1991).

CMB 8:00 am–10:00 am Room 316

Holographic Data Storage

Richard A. Linke, *NEC Research Institute Inc., President*

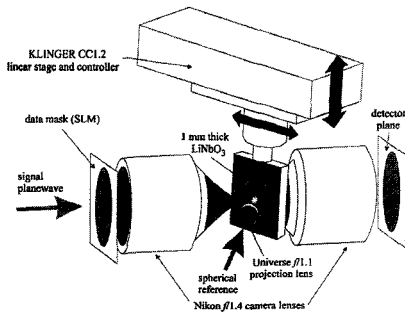
CMB1 8:00 am

Experimental demonstration of a holographic memory with a surface density of 100 bits/ μm^2

Allen Pu, Demetri Psaltis, *California Institute of Technology, Department of Electrical Engineering, 136-93 CALTECH, Pasadena, California 91125; E-mail: allenpu@sunoptics.caltech.edu*

The next generation compact disc due in early 1997, the Digital-Video-Disc (DVD), will have a capacity of ~ 6 Gbytes per layer, for a maximum planned capacity of ~ 20 Gbytes per double-sided disk with two layers on each side. That translates to a surface density of approximately 20 bits/ μm^2 for the four-layered DVD disk. In order for holographic three-dimensional disks to be competitive, we must demonstrate a much higher surface density than the most advanced DVD.

To demonstrate that a much higher surface density can be achieved holographically with a recording material similar in thickness to the compact disc, we constructed a holographic memory system using a 1-mm-thick LiNbO_3 (see Fig. 1). A pair of Nikon $f/1.4$, 3.9-cm-



CMB1 Fig. 1 Schematic diagram of a shift multiplexed, high density setup using a 1-mm-thick LiNbO_3 .

aperture camera lenses were used to image an E-beam lithographed chrome plated data mask to a CCD detector. A total of 590,000 pixels fit in the apertures of the two Nikon lenses, and a sharp image of the entire field was obtained at the detector plane. The center-to-center spacing of the pixels was $45 \mu\text{m}$ and the fill factor was 100%. The recording material, $2 \text{ cm} \times 2 \text{ cm} \times 1 \text{ mm}$ iron-doped LiNbO_3 was mounted on two translation stages for shift multiplexing.¹ Instead of recording the holograms with a planewave reference beam, a spherical reference beam was formed by using a $f/1.1$ projection lens. If a hologram recorded with a spherical reference beam is shifted slightly during reconstruction, the wavefront it experiences will be different from the wavefront used to record it. Therefore, the reconstruction will be suppressed and another hologram could be recorded, partially overlapping the previous hologram. For this experiment, horizontal displacement of the recording material (parallel to the plane of interaction) was provided by a Klinger CC1.2 linear stage and controller. Vertical displacement was provided by a manual translation stage. The holograms were recorded with the LiNbO_3 slightly past the Fourier transform plane of the Nikon lenses for a more uniform signal beam.

A surface density of $100 \text{ bits}/\mu\text{m}^2$ was achieved by storing 590,000 pixels in each hologram, over an effective hologram area of $5850 \mu\text{m}^2$ ($7.8 \mu\text{m}$ horizontal displacement \times 0.75 mm vertical displacement per hologram). The resulting estimated raw bit error rate (BER) was approximately 10^{-4} and no errors were observed in the sampled hologram when localized threshold values were used. At $100 \text{ bits}/\mu\text{m}^2$, we have a comfortable margin over the projected surface density of the most advanced DVD system. Furthermore, the results obtained from this experiment can be applied to a shift multiplexed holographic three-dimensional disk system. The capacity per 120-mm disk at $100 \text{ bits}/\mu\text{m}^2$ is approximately 100 Gbytes.

1. D. Psaltis, M. Levene, A. Pu, G. Barbastathis, K. Curtis, *Opt. Lett.* **20**, 782 (1995).

CMB2

8:15 am

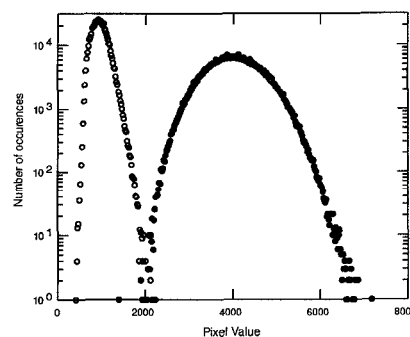
Megapixel imaging for high-performance holographic data storage

J. A. Hoffnagle, M.-P. Bernal, G. W. Burr, H. Coufal, R. K. Grygier, H. Günther, C. M. Jefferson, R. M. Macfarlane, R. M. Shelby, P. Wimmer, *IBM Research Division, Almaden Research Center, 650 Harry Road, San Jose, California 95120-6099*

Many potential advantages of holographic storage, including high volumetric data density, high data transfer bandwidth, and low latency time, derive from the simultaneous readout of large data pages, which lends itself to parallel processing. It is therefore important to maximize the data density per page. To date, demonstrations of holographic digital data storage have generally used detection oversampling, i.e., each data bit is sampled by several CCD pixels.¹⁻⁴ While this relaxes the requirements for optical alignment, it greatly increases the size and cost of the CCD, for a given data page size. Moreover, clocking out redundant CCD pixels increases the read time per page, and the algorithms needed to transform the oversampled CCD output to binary data require processing time and computational resources, adding to the cost of the system. Here we demonstrate imaging of 1 M pixel holographic data pages on a CCD camera in the limit of maximum data density, where every pixel corresponds to an independent data bit.

The experiments were performed on the IBM HOST test stand, described in detail elsewhere.⁵ The SLM was a chrome-on-glass mask, imaged by a pair of Fourier transform lenses with unit magnification onto a CCD camera having 1536×1024 pixels and 14-bit grey scale resolution. The data pattern on the SLM was a 1024×1024 array of random bits, with a pixel pitch of $9 \mu\text{m}$, matching that of the CCD. The holographic medium was located 3 cm behind the Fourier plane; for these experiments a $15 \times 15 \times 8 \text{ mm}$ crystal of LiNbO_3 doped with 0.02% Fe was chosen because of its excellent optical quality and availability with large clear aperture.

For every pixel of the CCD array to provide one bit of data, without oversampling, it is necessary that the image of the SLM be accurately pixel-matched to the CCD over the en-



CMB2 Fig. 1 Histograms of CCD pixel values for holographic readout of a 1 Mb data page stored in $\text{LiNbO}_3:\text{Fe}$. Open and closed circles denote 0 s and 1 s, respectively.

tire field of view. Imaging errors of a few tenths of a pixel cause unacceptable inter-pixel cross talk. For our 1024×1024 data array, this means that the magnification of the optical system must equal 1 to within $\sim 10^{-4}$, the SLM and CCD arrays must be parallel to within $\sim 0.1 \text{ mrad}$, and the image of the SLM must be registered on the CCD to within $\sim 0.9 \mu\text{m}$.

Figure 1 shows histograms of the CCD output for a reconstructed hologram, obtained with 90° geometry and 5-ms reference beam exposure. From the separation of 0 s and 1 s, one sees that the original data can be reconstructed with only 16 errors using a global threshold. With a simple local threshold, error-free readout of a megapixel page of holographic data, without oversampling, is possible.

1. J. F. Heanue, M. C. Bashaw, L. Hesselink, *Science* **265**, 749 (1994).
2. I. McMichael *et al.*, *Appl. Opt.* **35**, 2375 (1996).
3. A. Pu, D. Psaltis, *Appl. Opt.* **35**, 2389 (1996).
4. G. W. Burr *et al.*, submitted to *Opt. Lett.*
5. M.-P. Bernal *et al.*, *Appl. Opt.* **35**, 2360 (1996).

CMB3 (Invited)

8:30 am

Evaluation of holographic recording materials from a storage systems perspective

Glenn T. Sincerbox, M.-P. Bernal,* G. W. Burr,* H. Coufal,* R. K. Grygier,* J. A. Hoffnagle,* C. M. Jefferson,* R. M. Macfarlane,* R. M. Shelby,* *Optical Sciences Center, University of Arizona, Tucson, Arizona 85721*

To successfully compete with currently available data storage technologies such as magnetic disk, tape and the many variants of optical recording (CD-ROM, CD-R, CD-E, magneto-optic, DVD, etc.), holographic storage must provide significant performance and cost advantages to attract the end-user. The capacity of the system, be it the capacity of a page or of the entire system, is a critical factor in determining the data rate and the overall cost per megabyte of the system. These are, in turn, determined to a large extent by the reliability of storage, more correctly; the reliability of retrieval as measured by the bit error rate (BER). The goal is to push the capacity to the limit of minimum acceptable BER allowing for appropriate margins in component variability and long-term drift.

Many factors contribute in determining the BER of a holographic storage system including; the number of bits and physical size of the data page, the number of data pages multiplexed in a common recording volume, the multiplexing method, uniformity of illumination, the physical size of the hologram, the contrast of the input page composer or spatial light modulator, scattered light, detector integration time and detector noise. Some of these are systems considerations and others such as scattering, optical quality and recording dynamic range are intrinsic to the recording material. In the case of photorefractive materials,